Undergraduate Journal of Experimental Microbiology and Immunology (UJEMI) Vol. 29:1-10

Construction of a Plasmid that Expresses an N-terminally 6xHis Tagged Protein Spanning Amino Acids Gly139 to Pro552 of the Passenger Domain of the *Escherichia coli* Autotransporter Protein Ag43

Rachel Leong, Sina Safaeian, Jenny Zhang

Department of Microbiology and Immunology, University of British Columbia, Vancouver, British Columbia, Canada

SUMMARY *Escherichia coli*, a Gram-negative bacterium, exhibits resistance to multiple antibiotics, emphasising the need for novel targets. Autotransporter (AT) proteins, such as Antigen 43 (Ag43), have emerged as potential targets due to their association with virulence. Autotransporters are a family of secreted proteins in Gram-negative bacteria, and Ag43, with its modular structure, plays a prominent role. This study focuses on the secreted passenger domain of Ag43. Previous research suggested that the autochaperone, a conserved amino acid sequence located at the C-terminus of many autotransporter passengers, is required for proper passenger domain folding during secretion. Our goal was to investigate the role of the so called autochaperone domain in the Ag43 passenger sequence. Our study aimed to create recombinant plasmids that would enable expression, purification, and refolding of Ag43 passenger domain variants with and without the putative autochaperone region. Using PCR and standard cloning techniques, we were able to create a plasmid termed pXYZ encoding an N-terminally tagged Ag43 passenger lacking the autochaperone region (amino acid X to amino acid Y). We were unable to create a plasmid encoding Ag43 containing the autochaperone region. Follow-up analyses using SDS PAGE showed that Ag43 (lacking the autochaperone region) is expressed in the cytosol of *E. coli* strain BL21. This project lays the building blocks for investigating the role of the autochaperone region in Ag43 folding and the effector function of Ag43 in order to characterise the motif as a potential novel antimicrobial target.

INTRODUCTION

Autotransporters (ATs) are a family of secreted proteins in Gram-negative bacteria such as *Escherichia coli* and are frequently correlated with virulence in all *E. coli* pathotypes. Autotransporters consist of a single polypeptide which mediates the transport of the protein across both the inner and outer bacterial membrane (1). A subclass of autotransporters is the type V secretion system in which all information necessary for crossing the membrane is included in the protein itself (2). The translocation of type V AT across these membranes has been implicated with the proteins' N-terminal passenger domain and C-terminal translocation domain (3, 4). Based on prior research, we know that, in particular, autochaperone (AC) motifs found at the C-terminal ends of AT passenger domains are critical to the correct folding of the passenger region both at the bacterial surface and in vitro (5).

The autochaperone is defined as the functional unit at the C-terminus of the passenger domain of autotransporters, capable of catalysing passenger folding and efficient OM translocation (5). Before the term "autochaperone" was coined, Ohnishi et al. (1994) found that the deletion of the junction region between the mature protease and processed COOH-terminal protein of the *Serratia marcescens* serine protease (PrtS) resulted in the lack of detection of the protein in any fractions of the cells or in the medium, but with the COOH-terminal protein in the outer membrane (6). Oliver et al. then found that a region within the BrkA passenger was necessary for its folding and suggested that the conservation of the AC junctions' conservation would allow similar results to be found in other ATs (7) Since then, AC regions have been identified in EspP, Tsh, AIDA-I, Hbp, and IcsA (8–15). The AC region

Published Online: September 2024

Citation: Leong, Safaeian, Zhang. 2024. Construction of a plasmid that expresses an N-terminally 6xHis tagged protein spanning amino acids Gly139 to Pro552 of the passenger domain of the *Escherichia coli* autotransporter protein Ag43. UJEMI 29:1-10

Editor: Shruti Sandilya and Ronja Kothe, University of British Columbia

Address correspondence to: https://jemi.microbiology.ubc.ca/

has been confirmed to be a conserved structure across multiple ATs, specifically with sequence analysis of 1523 ATs identifying ACs in the majority of self-associating ATs (16) such as Ag43.

Ag43, also known as Antigen 43, is an AT protein prominently found on the surface of a majority of *E. coli* strains (17, 18). Hallmarks of Ag43 include its phase-variable expression, its three-domain AT structure and its functions associated with biofilm formation, aggregation, and self-recognizing adhesion to the host cell (19). Specifically, due to the ability of Ag43 to aggregate, the protein also expresses auto-aggregation or aggregation with itself, observed as the formation of bacterial clumping and fluffing of the same cells at the bottom of culture tubes (20, 21). The modular structure of Ag43 consists of a signal peptide which directs translocation across the cytoplasmic membrane, a passenger domain, an autochaperone domain, and an outer membrane translocator (Figure 1) (18). It is a self-associating AT that is synthesised as a 1039 amino acid preprotein (19). Studies have shown that Ag43 likely possesses a conserved AC region homologous to those found in other ATs (16). Furthermore, the specific function and importance of the AC region in Ag43 has not yet been experimentally confirmed.

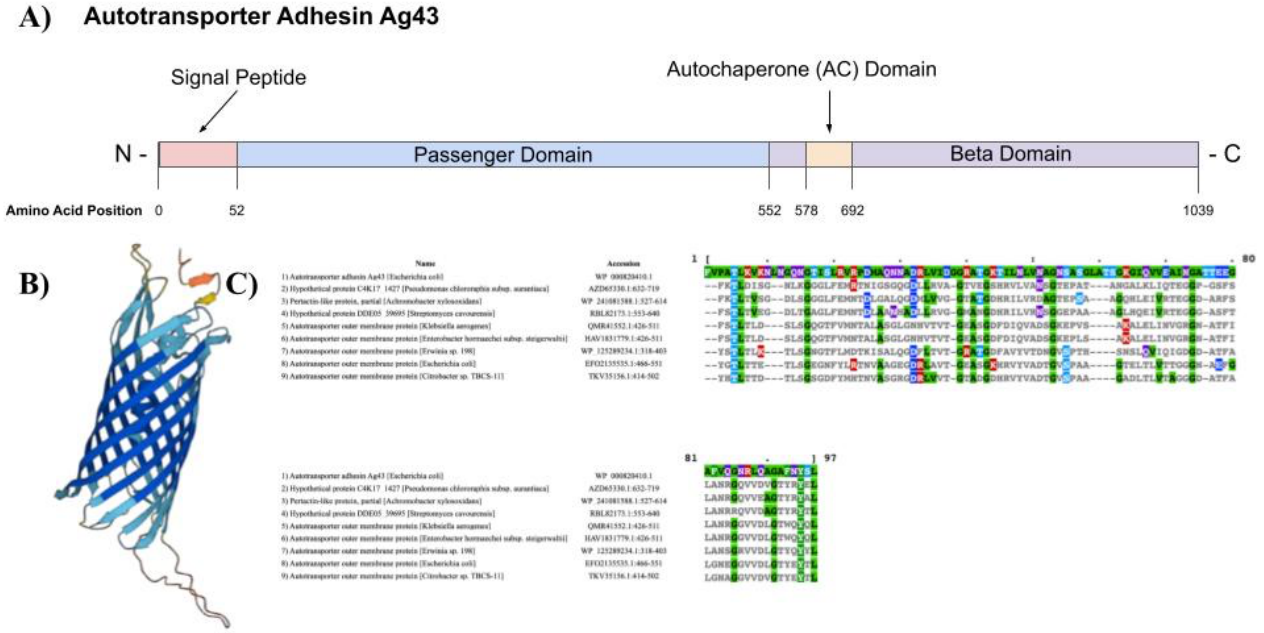

FIG. 1 Domain structure of Ag43. (A) Protein domain map of autotransporter adhesin Ag43 cloned from *E. coli*. (B) The folded tertiary structure of *E. coli* Ag43 adapted from Alphafold (22, 23).

This study establishes building blocks for a proposed study design aiming to determine the functional importance of the conserved AC region within the passenger domain. Such building blocks include successfully designing primers for amplification of the Ag43 constructs, choosing restriction endonucleases and designing protocols for restriction, cleavage and ligation. We constructed a plasmid, pEEKABOO, which removes the AC region from the Ag43 plasmid and we lay out the procedures for construction of an additional plasmid that includes the AC region. Our study can be built upon to potentially provide a novel antibacterial target for antimicrobial-resistant pathogens.

METHODS AND MATERIALS

Cell culture, strains, and plasmids. The pBAD-Ag43 plasmid bearing the *E. coli* Ag43 was obtained from AddGene (22) while the pET-28a(+) destination vector was obtained from the University of British Columbia's Department of Microbiology (UBC MBIM). Competent DH5α *E. coli* cells were obtained from ThermoFisher© (Cat. #EC0112), and BL21(DE3) *E. coli* cultures were obtained from UBC MBIM. Liquid cultures were all grown in Luria Bertani (LB) medium (23) with the addition of 100 mg/mL ampicillin (for cells carrying pBAD-Ag43) or 50 mg/mL Kanamycin (for cells bearing a pET-28a based plasmid) as the selection

marker (24). Plate cultures of cells were grown on the same recipes for LB but with the addition of 1.5% W/W Agar-Agar (23). Super Optimal Broth (SOC) (25) was used as the recovery medium following transformations. All growth was at 37°C and a shaker was used for liquid cultures.

PCR primer design. Custom DNA primers were designed for the desired amplicons (the passenger region of the Ag43 gene lacking the proposed autochaperone region $^{\text{Glycine-139 to Proline-552}}$) using SnapGene™ (www.snapgene.com). The length of the complementary region between primers and the template region on pBAD-Ag43 was adjusted to produce a predicted melting point around 50-60 °C as per American Society of Microbiology (ASM) suggestions (26) and HindIII and XhoI restriction enzyme cut sites were integrated into the forward and reverse primers to make directional insertion into the destination vector possible. A poly-A tail was added to end of each primer to meet enzyme cut site requirements (27).

PCR and amplicon purification. PCR amplification of the passenger region of the Ag43 gene lacking the proposed autochaperone region was performed using ThermoFisher™ Recombinant Taq Polymerase (Cat #EP0402) as per manufacturer guidelines (28). PCR products were purified via the QiaQuick PCR Cleanup Kit (Cat. #28104). PCR products were visualised via gel electrophoresis to confirm specificity of reaction and size.

Nucleic acid purification. Plasmid purification was performed on overnight cultures of DH5a *E. coli* cells using the BioBasic EZ-10 Plasmid Purification MiniPrep kit (Cat. #BS414) as per manufacturer guidelines for a low copy number plasmid (29). Purification of PCR products and restriction digest products were done using the Qiagen QiaQuick PCR Purification Kit (Cat. #28104) as per manufacturer protocol (30).

DNA gel electrophoresis. Purified DNA samples were mixed in a 5:1 ratio with 6x DNA loading dye from ThermoFisher (Cat. #R0611) and run on a 1% agarose gel made as per the protocol by Froggabio (31). Gels were run for 1 hour at 120 volts. ThermoFisher GeneRuler 1 kb (Cat. #SM0311) was used as a ladder. Gels were visualised on a Bio-Rad GelDoc© system (32).

SDS Protein gel electrophoresis and visualisation. Total cell lysate samples were produced through centrifuging 100 uL of BL21(DE3) cells expressing the desired protein; the supernatant was removed, and the pellets were resuspended in 100 uL of 2x Laemelli buffer (Bio-Rad Cat. #1610737) before boiling for 5 minutes ate 95 °C. Mixture was centrifuged momentarily to pull down condensation. 15 uL of sample was loaded into a 10% BioRad Mini-PROTEAN TGX pre-cast SDS gel (Cat. #4561036) and run in the BioBasic Mini-PROTEAN TetraCell (Cat. #1658000) as per manufacturer specifications (33). BioRad Precision Plus Protein Unstained Standards (Cat. #1610363) was used as a ladder. Gels were visualised on a Bio-Rad GelDoc© system.

Restriction digestion. The destination vector, pET-28a(+), was purified and digested with the restriction enzymes, HindIII and XhoI as per double digest protocols listed by New England Biolabs (NEB) (34). The amplified Ag43 passenger lacking the autochaperone region was also digested with HindIII and XhoI (34). The digested pET-28a(+) vector was purified of the excised fragment.

Plasmid construction and selection. The purified digested pET-28a(+) vector and digested Ag43 passenger minus the autochaperone amplification product were ligated using NEB's T4 DNA Ligase (Cat #M0202) as per manufacturer instructions (35). Ligation products were immediately transformed into competent DH5α *E. coli* cells as per vendor protocols and plated on 100 mg/mL ampicillin and 50 mg/mL kanamycin plates respectively (36). Transformants colonies were picked at random from selection plates and grown overnight at 37°C. The pEEKABOO plasmid was purified from the overnight culture and a sample of it was double digested with HindIII and XhoI. Digestion productions were visualised on an

agarose gel to check for presence of bands corresponding to the utilised destination vector (approximately 5.2 kB) and desired DNA insert (approximately 1.3 kB).

Plasmid Sequencing. Whole plasmid sequencing of plasmids isolated from selected transformants was done through a commercial vendor, Plasmidsaurus™.

Expression of recombinant protein. For protein expression, competent BL21(DE3) *E. coli* cells were transformed with pEEKABOO constructs as per standard protocols from the Hancock Lab at UBC MBIM (37); recovery medium was switched to SOC. The following day, 3 transformant colonies was selected and induced with Isopropyl ß-D-1-thiogalactopyranoside (IPTG) to begin expressing recombinant Ag43 passengerΔautochaperone protein as per procedures from Biologics International (38). Expression was confirmed via SDS gel electrophoresis of total cell protein.

RESULTS

In this study, primers for Ag43 were designed and tested on Snapgene, and restriction endonucleases for the pET-28a(+) plasmid were selected to amplify two Ag43 constructs: Ag43passenger and Ag43passenger without the autochaperone region (Ag43passengerΔautochaperone). Amplification involved a denaturation step and three-step temperature cycle, which produced successful results of the constructs that were visualised on a 1% agarose gel (Figure 2).

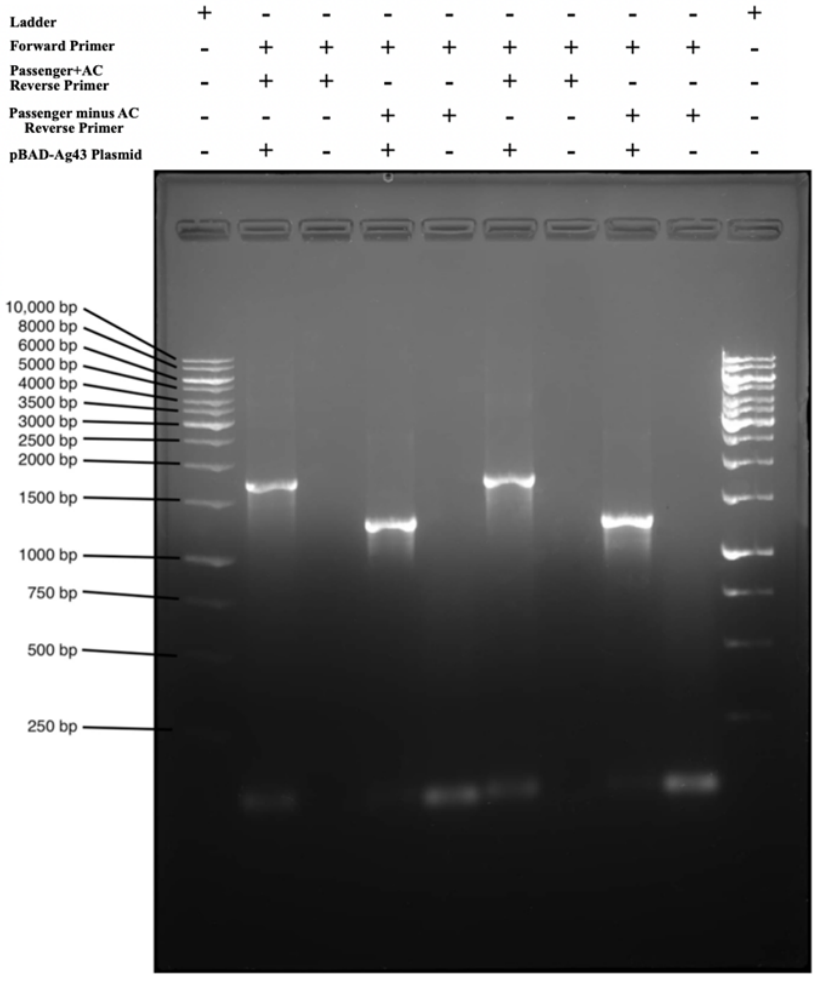

FIG. 2 A 1% agarose gel confirms correct PCR amplification of the Ag43 passenger subdomain, with and without the AC subdomain using custom primers. Custom primers for amplifying the Ag43 passenger domain sequence, with and without the AC subdomain, while also integrating cut sites for the HindIII and XhoI enzymes at the 5' and 3' ends of the amplicon, respectively. Lanes 1/10 are ladder. Lanes 2/6 both show a ~1700 bp amplification product from using the primer set for amplifying the whole Ag43 passenger domain, with lanes 3/7 visualising their negative controls. Lanes 4/8 both show a ~1300 bp amplification product from using the primer set for amplifying the Ag43 passenger minus the autochaperone subdomain, with lanes 5/9 visualising their negative controls.

The pET-28a(+) plasmid was cleaved with restriction enzymes HindIII-HF and XhoI for ligation with the Ag43 constructs to create pEEKABOOwAC (pET28-Ag43passenger) and pEEKABOO (pET-28Ag43passengerΔautochaperone). After the incubation and ligation, each construct was heat-inactivated and chilled at 4°C for storage. Transformation into DH5a *E. coli* cells, which were observed to be circular and even, was

performed to produce colonies for plasmid extraction. The plasmid extracted products were double digested with HindIII-HF and Xho1, then visualised via gel electrophoresis (Figure 3). The double digested pEEKABOOwAC constructs (lanes 3 and 11, Figure 3) were expected to show bands at ~7000, ~5500, and ~1700 bp, however only a band at ~5200 bp was observed. The double digested pEEKABOO constructs (lanes 5 and 13, Figure 3) were expected to show bands at ~6600 bp, ~5200 bp, and ~1300 bp, however only bands at ~6600 bp and ~5200 bp were visible through the gel. Both the destination vector (lane 7, Figure 3) and control vector (lane 9, Figure 3) showed their expected bands through the gel.

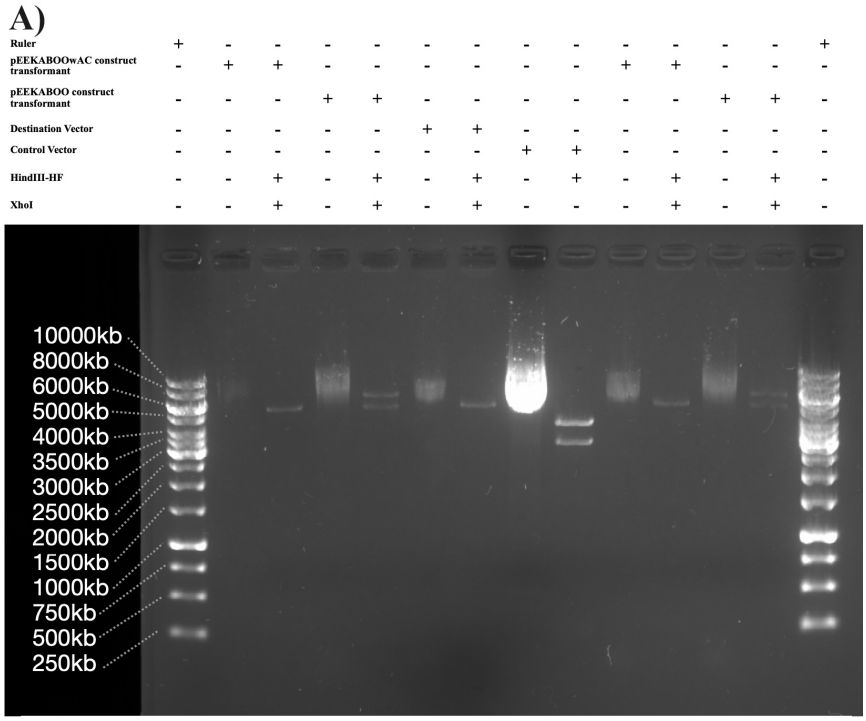

FIG. 3 Double restriction enzyme digestion with HindIII and XhoI used to select for the pEEKABOO construct. A) A 1% agarose gel was used to visualise the outcome of the double digest. pEEKABOO is comprised of a ~1.3 kBp insert within a ~5.2 kBp destination vector. B) Graphical view of the pEEKABOO plasmid as confirmed via whole plasmid sequencing.

The pEEKABOOwAC construct selected from Figure 3 was sequenced via Plasmidsaurus™, validating that our construct precisely matches the planned design. Specifically, the plasmid contains the segment from glycine-139 to proline-552 of the Ag43 gene inserted between the HindIII and XhoI cut sites in the multiple cloning site (MCS) of the pET-28a(+) destination vector (Supplemental Figure S1).

The pEEKABOO construct was transformed into BL21(DE3) *E. coli* cells and induced with IPTG. The pEEKABOO constructs were then grown in LB with 1 mM IPTG for 3-4 days with a negative control of pEEKABOO constructs without IPTG. IPTG was used to allow blocking of the expression inhibition on T7 promoters. In the absence of IPTG, the lac repressor binds to the lac operator, which inhibits the transcription of downstream genes. Thus, by inducing our constructs with IPTG, IPTG would alleviate expression inhibition on the T7 promoters to allow for transcription of downstream genes. These constructs were then visualised via SDS gel electrophoresis (Figure 4). The results shown in the gel were as expected, with brighter prominent bands at just under 50 kD with pEEKABOO grown in IPTG (lanes 4, 5, 8, 9, 12, and 13, Figure 4). The brighter bands in negative control lanes 3, 7, 11 (Figure 4) are observed due to erroneous artifacting. The brighter banding with the IPTG induced lanes demonstrates that more of the downstream genes were transcribed in comparison to the negative control, which was as expected.

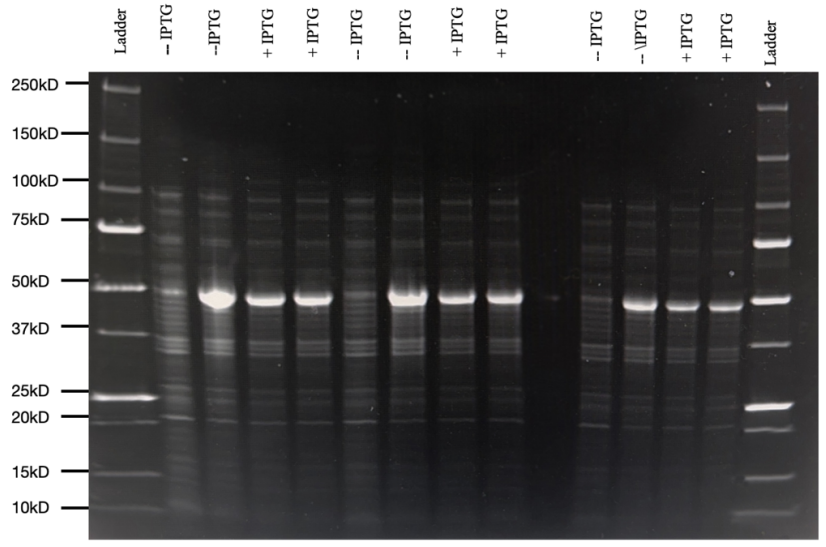

FIG. 4 BL21(DE3) *E. coli* transformed with pEEKABOOwACΔautochaperone can be induced with IPTG to produce recombinant Ag43 protein passenger minus the AC subdomain. Competent BL21(DE3) *E. coli* were transformed with pEEKABOOwACΔautochaperone and grown in LB ± 1mM IPTG for 3-4 days before total cell lysates were visualised on an SDS gel. Lanes 1/14 are Bio-Rad Precision Plus Protein Unstained Standards. Lanes 2/3/6/7/11/12 are total cell lysates from un-induced BL21(DE3) *E. coli* cells bearing the pEEKABOOwACΔautochaperone plasmid. Lanes 4/5/8/9/12/13 are total cell lysates from BL21(DE3) E. coli cells bearing the pEEKABOO plasmid that were induced with IPTG.

DISCUSSION

In this study, the first steps of the proposed study design aimed at elucidating the effect of the AC region on secretion and folding are performed, most notably the creation of the pEEKABOO plasmid lacking the AC region. Primers were chosen to target the Ag43 passenger with and without the autochaperone subdomain (Figure 2), and digestion and ligation protocols were used to attempt to produce the pEEKABOOwAC and pEEKABOO constructs. A double digest was used to confirm the constructs, with the results for pEEKABOO nearly mirroring those expected based on SnapGene simulations with the exception of missing a band at 1300 bp (Figure 3). Whole plasmid sequencing on this construct confirmed its correctness (Supplementary Figure S2). However, the same was not able to be attempted with pEEKABOOwAC and remains to be done. In further characterising pEEKABOO, we transformed the plasmid into BL21(DE3) cells and induced the insert's expression with IPTG. The results aligned with our expectations, revealing brighter and prominent bands at ~50 kDa which is consistent with the predicted molecular size of the Ag43 passenger minus the autochaperone subdomain (Figure 4). However, it should be noted that one of the multiple negative control lanes exhibited an unexpectedly bright band around 50 kDa (Figure 4). This is believed to be due to artifacting given the aggregative properties of Ag43, technical issues such as uneven gel loading or improper sample preparation, or non-specific binding (39).

Limitations Chemical transformation of non-commercially competent BL21 *E. coli* cells requires BL21 *E. coli* cells to be suspended on ice for 1-40 hours, with an optimal time of 24 hours. However, due to time constraints, the suspended BL21 *E. coli* cells were left on ice for only 40 minutes. This could have led to low transformation efficiency and uptake of the pEEKABOO construct. Future experiments should follow the optimal measurements and timing of the CMDR transformation of cells protocol (37). Furthermore, although the pEEKABOOconstruct was well characterised in this study through double digestion, transformation, IPTG induction, and gel visualisation, the pEEKABOOwAC construct has yet to be characterised. Similar experiments should be performed on the pEEKABOOwAC construct by future groups.

Conclusions In this study, we designed primers, restriction enzymes and appropriate protocols for the creation of the pEEKABOO plasmid and then subsequently created said plasmid. We propose study designs as future directions that build upon this work in order to characterise the effect of the AC region on Ag43 protein secretion and folding on the outer membrane of bacterial cells. Our results show successful amplification, cleavage, ligation and transformation of the desired plasmid and preliminary results showing the successful production of the Ag43 protein without the AC region. Further future studies building on our work include characterising AC driven protein folding and assessing the effector function of the AC and 'α' regions of the Ag43 protein on agglutination. Our results provide further confirmation of the conservation of the autochaperone region and put forth a viable novel therapeutic target for combating antimicrobial resistance.

Future Directions Our successful amplification protocol design and cleavage-and-ligation protocols build the groundwork for potential future projects characterising the autochaperone domain in regards to autotransporter secretion and function. In this study we successfully constructed the pEEKABOO construct: a plasmid bearing the Ag43 AT lacking the AC subdomain under the control of a T7 promoter and observed protein expression. Since AC regions are important for protein folding (12) we will utilise our pEEKABOO construct to investigate how the Ag43 AC is associated with protein folding. The current study handles the design of the PCR primers and restriction endonuclease enzymes for the plasmid pET-28a(+) destination vector; the PCR amplification; the cleavage and ligation with the restriction endonuclease enzymes Hind-III and XhoI into the destination vector; and the culturing and transformation of the constructed plasmids into competent *E. coli* DH5α and subsequent BL21 cells. Our proposed study design is a continuation of these completed steps. The most subsequent course of action would be to proceed with the processing of the pEEKABOOwAC construct to produce said construct and confirm its expression with a protocol similar to that which we performed for pEEKABOO. Following this would be lysing the transformed cells and purifying in order to obtain properly folded inclusion bodies from the strains, done with a nickel column. The 6xHis amino acid tags such as the one within the construct created in this study are able to bind nickel NTA columns while proteins without them cannot. Then, the Ag43 gene translated into the inclusion bodies as part of this construct should be obtained and purified based on the presence of this 6xHis tag. A dialysis would follow in order to clean or remove any unwanted compounds from the sample and allow proteins to fold properly. A trypsinization assay would then finally be run to confirm protein folding and thus the effect of the autochaperone domain. We hypothesise that deletion of the autochaperone region from the Ag43 passenger domain will inhibit proper folding of the Ag43 protein passenger region. If the proposed subsequent steps are followed and executed properly, we expect an eluted mixture containing a purified sample of the 6xHis tagged Ag43 protein upon lysis and purification. If the autochaperone is sufficient for proper passenger folding, the protein will refold in the dialysis assay. These passenger domains will be cleaved upon trypsinization, and should present a band of approximately 63 kDa with the autochaperone region and 47 kDa without.

Additionally, testing a construct that only expresses the non-AC portion of the Ag43 passenger, dubbed the 'α' domain, provides a unique opportunity to study Ag43's effector function. Therefore, we would assess whether the recombinant form of the Ag43 passenger

fragment expressed by our construct is sufficient to induce the agglutination of *E. coli* in solution. Recent work in this field has shown that the deletion of the tail 358 amino acid residues from the 'α' subdomain of Ag43 (Ag43α) does not negatively impact its effector functionality and that cells expressing the altered protein still agglutinate when growing in liquid medium (Mazariegos et al., personal communication). This confirms that *E. coli* expressing just the 'α' subdomain of Ag43 retain the ability to auto-aggregate (40). In turn, we believe it is important to study whether the addition of autogenous Ag43α into a liquid medium can trigger non-agglutinating *E. coli* strains to do so. The first step to doing this would be to attempt overexpression of the Ag43α peptide from the Ag43α bearing pET construct and to isolate the protein using the 6xHis tag and nickel affinity chromatography (7). From there, liquid cultures of one or more non-agglutinating species of *E. coli* would be inoculated with the Ag43α protein at various dilutions to observe changes to bacterial aggregation and possibly branching from here to further ask whether the protein can induce the agglutination of gram-negative bacteria beyond *E. coli*, as characteristics of bacterial cell walls are widely conserved. The main applications of this research would be in the food and water treatment industries, where natural and biodegradable flocculants for the removal of suspended microbial matter are desired to reduce the environmental impact and toxicity associated with the use of synthetic flocculants (41). Lastly, the growing body of research into bacteria-derived subunit vaccines in the fight against antibacterial resistance prompts the question of whether a subunit vaccine displaying Ag43α would be able to impede the establishment of urinary tract infections by certain uropathogenic *E. coli* strains that rely on the activity of Ag43 for virulence (42, 43). This would be through triggering IgA-based humoral mucosal immunity with antibodies that can neutralise Ag43, similar to the mechanism of action utilised by Valneva SE's Dukoral vaccine against gastrointestinal infection with *Vibrio cholerae* (44).

ACKNOWLEDGEMENTS

We would like to acknowledge the MICB 471 teaching team, Dr. David Oliver, Jade Muileboom, and Charlotte Clayton for their constant support on this project. Dr. Oliver's guidance and knowledge were crucial for the success of this project. The team expresses their appreciation for Jade Muileboom's expertise in the lab and help with troubleshooting, and Charlotte Clayton's suggestions and edits for this manuscript. Our team would also like to thank the Department of Microbiology and Immunology at the University of British Columbia Vancouver for providing the funding and resources for this course and our invaluable research experience.

CONTRIBUTIONS

All authors contributed equally to the study design and experimentation. References and the introduction were contributions of R.L.; methods and figures were done by S.S., and the results and abstract were written by J.Z. All authors contributed to the discussion, editing, and reviewing of the paper. The idea of the project was crafted by S.S.

REFERENCES

1. **Leo JC, Grin I, Linke D**. 2012. Type V secretion: mechanism(s) of autotransport through the bacterial outer membrane. *Philos Trans R Soc B Biol Sci* **367**:1088–1101.
2. **Bouguénec CL**. 2005. Adhesins and invasins of pathogenic *Escherichia coli. Int J Med Microbiol* **295**:471–478.
3. **Bernstein HD**. 2015. Looks can be deceiving: recent insights into the mechanism of protein secretion by the autotransporter pathway: Recent insights into autotransporter secretion. *Mol Microbiol* **97**:205–215.
4. **Fan E, Chauhan N, Udatha DBRKG, Leo JC, Linke D**. 2016. Type V secretion systems in bacteria. *Microbiol Spectr* **4**:4.1.10.
5. **Drobnak I, Braselmann E, Chaney JL, Leyton DL, Bernstein HD, Lithgow T, Luirink J, Nataro JP, Clark PL**. 2015. Of linkers and autochaperones: an unambiguous nomenclature to identify common and uncommon themes for autotransporter secretion. *Mol Microbiol* **95**:1–16.

6. **Ohnishi Y, Nishiyama M, Horinouchi S, Beppu T**. 1994. Involvement of the COOH-terminal pro-sequence of *Serratia marcescens* serine protease in the folding of the mature enzyme. *J Biol Chem* **269**:32800–32806.
7. **Oliver DC, Huang G, Nodel E, Pleasance S, Fernandez RC**. 2003. A conserved region within the *Bordetella pertussis* autotransporter BrkA is necessary for folding of its passenger domain: conserved autotransporter domain necessary for folding. *Mol Microbiol* **47**:1367–1383.
8. **Velarde JJ, Nataro JP**. 2004. Hydrophobic residues of the autotransporter EspP linker domain are important for outer membrane translocation of its passenger. *J Biol Chem* **279**:31495–31504.
9. **Kang'ethe W, Bernstein HD**. 2013. Stepwise folding of an autotransporter passenger domain is not essential for its secretion. *J Biol Chem* **288**:35028–35038.
10. **Kostakioti M, Stathopoulos C**. 2006. Role of the α-helical linker of the C-terminal translocator in the biogenesis of the serine protease subfamily of autotransporters. *Infect Immun* **74**:4961–4969.
11. **Berthiaume F, Rutherford N, Mourez M**. 2007. Mutations affecting the biogenesis of the AIDA-I autotransporter. *Res Microbiol* **158**:348–354.
12. **Soprova Z, Sauri A, Van Ulsen P, Tame JRH, Den Blaauwen T, Jong WSP, Luirink J**. 2010. A conserved aromatic residue in the autochaperone domain of the autotransporter Hbp is critical for initiation of outer membrane translocation. *J Biol Chem* **285**:38224–38233.
13. **Teh MY, Tran ENH, Morona R**. 2012. Absence of O antigen suppresses *Shigella flexneri* IcsA autochaperone region mutations. *Microbiol* **158**:2835–2850.
14. **Kühnel K, Diezmann D**. 2011. Crystal structure of the autochaperone region from the *Shigella flexneri* autotransporter IcsA. *J Bacteriol* **193**:2042–2045.
15. **Thanassi DG, Stathopoulos C, Karkal A, Li H**. 2005. Protein secretion in the absence of ATP: the autotransporter, two-partner secretion and chaperone/usher pathways of Gram-negative bacteria (Review). *Mol Membr Biol* **22**:63–72.
16. **Rojas-Lopez M, Zorgani MA, Kelley LA, Bailly X, Kajava AV, Henderson IR, Polticelli F, Pizza M, Rosini R, Desvaux M**. 2018. Identification of the autochaperone domain in the type Va secretion system (T5aSS): prevalent feature of autotransporters with a β-helical passenger. *Front Microbiol* **8**:2607.
17. **Van Houdt R, Michiels CW**. 2005. Role of bacterial cell surface structures in *Escherichia coli* biofilm formation. *Res Microbiol* **156**:626–633.
18. **Ageorges V, Wawrzyniak I, Ruiz P, Bicep C, Zorgani MA, Paxman JJ, Heras B, Henderson IR, Leroy S, Bailly X, Sapountzis P, Peyretaillade E, Desvaux M**. 2023. Genome-wide analysis of antigen 43 (Ag43) variants: new insights in their diversity, distribution and prevalence in bacteria. *Int J Mol Sci* **24**:5500.
19. **Wells TJ, Tree JJ, Ulett GC, Schembri MA**. 2007. Autotransporter proteins: novel targets at the bacterial cell surface. *FEMS Microbiol Lett* **274**:163–172.
20. **Schembri MA, Hjerrild L, Gjermansen M, Klemm P**. 2003. Differential expression of the *Escherichia coli* autoaggregation factor antigen 43. *J Bacteriol* **185**:2236–2242.
21. **Trunk T, S. Khalil H, C. Leo J, Bacterial Cell Surface Group, Section for Genetics and Evolutionary Biology, Department of Biosciences, University of Oslo, Oslo, Norway.** 2018. Bacterial autoaggregation. *AIMS Microbiol* **4**:140–164.
22. **Jin X, Riedel-Kruse IH**. 2018. Biofilm lithography enables high-resolution cell patterning via optogenetic adhesin expression. *Proc Natl Acad Sci U S A* **115**:3698–3703.
23. **MacWilliams MP, Liao M-K**. 2006. Luria Broth (LB) and Luria Agar (LA) media and their uses protocol. American Society for Microbiology.
24. **Griffits Lab**. 2023. Stock Solution. Department of Microbiology and Molecular Biology, Brigham Young University.
25. 2023. What is the recipe for SOC medium? QIAGEN. https://www.qiagen.com/us/resources/faq?id=d3be05d0-ec02-4ced-aabe-dcd2a1061920&lang=en. Retrieved 18 December 2023.
26. **Suchman E**. 2011. Polymerase Chain Reaction protocol. American Society for Microbiology.
27. Cleavage close to the end of DNA fragments. Usage Guidel. New England BioLabs. https://www.neb.com/en/tools-and-resources/usage-guidelines/cleavage-close-to-the-end-of-dna-fragments#:~:text=Note%3A%20As%20a%20general%20rule,primer%20dimers%20are%20not%20formed. Retrieved 18 December 2023.
28. Taq DNA Plymerase. Thermo Fisher Scientific.
29. 2019. EZ-10 Spin Column Handbook. Bio Basic.
30. 2020. QIAquick Spin Handbook. QIAGEN.
31. RedSafe Nucleic Acid Staining Solution. iNtRON Biotechnology.
32. **McEllistrem MC, Stout JE, Harrison LH**. 2000. Simplified protocol for pulsed-field gel electrophoresis analysis of *Streptococcus pneumoniae*. *J Clin Microbiol* **38**:351–353.
33. 2011. Mini-PROTEAN Precast Gels: Instruction Manual and Application Guide. Bio-Rad Laboratories.
34. 2023. NEBcloner (1.13.10). New England BioLabs.
35. 2023. Ligation protocol with T4 DNA ligase (M0202). N Engl BioLabs. https://www.neb.com/en/protocols/0001/01/01/dna-ligation-with-t4-dna-ligase-m0202#:~:text=For%20cohesive%20(sticky)%20ends%2C,in%20a%2010%20minute%20ligation. Retrieved 18 December 2023.
36. 2019. DH5a competent cells. Thermo Fisher Scientific.

37. 2023. CaCl2 transformation of *E.coli.* R.E.W. Hancock Lab.
38. IPTG Induction Protocol. Biologics International Corp. https://www.biologicscorp.com/blog/iptg-induction-protocol/#:~:text=Fast%20IPTG%20induction%20protocol&text=Dilute%201%3A50%20(1%3A,in%20labeled%201.5ml%20tubes.
39. **Kurien BT, Scofield RH**. 2019. Artifacts and common errors in protein gel electrophoresis, p. 511–518. *In* **Kurien BT, Scofield RH** (eds.), Electrophoretic Separation of Proteins. Springer New York, New York, NY.
40. **Klemm P, Hjerrild L, Gjermansen M, Schembri MA**. 2004. Structure-function analysis of the self-recognizing Antigen 43 autotransporter protein from *Escherichia coli*. *Mol Microbiol* **51**:283–296.
41. **Santos A, Luz L, Napoleao T, Paiva P, Coelho L**. 2014. Coagulation, flocculation, agglutination and hemaglutination: similar properties? Advances in chemistry research. Volume 20. Nova Science Publishers, Incorporation, [Hauppauge], New York.
42. **Frost I, Sati H, Garcia-Vello P, Hasso-Agopsowicz M, Lienhardt C, Gigante V, Beyer P**. 2023. The role of bacterial vaccines in the fight against antimicrobial resistance: an analysis of the preclinical and clinical development pipeline. *Lancet Microbe* **4**:e113–e125.
43. **Zalewska-Pia̧tek B, Pia̧tek R, Olszewski M, Kur J**. 2015. Identification of antigen Ag43 in uropathogenic *Escherichia coli* Dr+ strains and defining its role in the pathogenesis of urinary tract infections. *Microbiol* **161**:1034–1049.
44. **Sirskyj D, Kumar A, Azizi A**. 2016. Mechanisms underlying the immune response generated by an oral Vibrio cholerae vaccine. *Int J Mol Sci* **17**:1062.
45. **Jumper J, Evans R, Pritzel A, Green T, Figurnov M, Ronneberger O, Tunyasuvunakool K, Bates R, Žídek A, Potapenko A, Bridgland A, Meyer C, Kohl SAA, Ballard AJ, Cowie A, Romera-Paredes B, Nikolov S, Jain R, Adler J, Back T, Petersen S, Reiman D, Clancy E, Zielinski M, Steinegger M, Pacholska M, Berghammer T, Bodenstein S, Silver D, Vinyals O, Senior AW, Kavukcuoglu K, Kohli P, Hassabis D**. 2021. Highly accurate protein structure prediction with AlphaFold. *Nature* **596**:583–589.
46. **Varadi M, Anyango S, Deshpande M, Nair S, Natassia C, Yordanova G, Yuan D, Stroe O, Wood G, Laydon A, Žídek A, Green T, Tunyasuvunakool K, Petersen S, Jumper J, Clancy E, Green R, Vora A, Lutfi M, Figurnov M, Cowie A, Hobbs N, Kohli P, Kleywegt G, Birney E, Hassabis D, Velankar S**. 2022. AlphaFold Protein Structure Database: massively expanding the structural coverage of protein-sequence space with high-accuracy models. *Nucleic Acids Res* **50**:D439–D444.